Analysis of the Substrate Uptake and Release Reactions of the Light-Driven Sodium-Pump Rhodopsin

(光駆動ナトリウムポンプロドプシンによる基質の取込み・放出反応の解析)

Graduate School of Life Science

Hokkaido University

2021.3

Keisuke Murabe

CONTENTS

ABBREVIATIONS

- CCCP carbonyl cyanide m-chlorophenyl hydrazine
- CP Cytoplasmic
- DDM n-dodecyl β-D-maltopyranoside
- EC Extracellular
- *E. coli* *Escherichia coli*
- GLR NaR from the eubacterium *Gillisia limnaea*
- K_d Dissociation constant
- λmax Absorption maximum wavelength
- NaR Na^+ pump rhodopsin
- NPOE o-nitrophenyloctylether
- PC Phosphatidylcholine
- PR Proteorhodopsin
- PSB Protonated Schiff base
- PVC Polyvinyl chloride

ABSTRACT

For membrane transporters, substrate uptake and release reactions are major events during their transport cycles. Despite the functional importance of these events, it is difficult to identify their relevant structural intermediates because of the requirements of the experimental methods, which are to detect the timing of the formation and decay of intermediates and to detect the timing of substrate uptake and release. I report successfully achieving this for the light-driven Na^+ pump rhodopsin (NaR). Here, a Na^+-selective membrane, which consists of polyvinyl chloride and a Na^+ ionophore, was employed to detect Na^+ uptake and release. Firstly, I confirmed the Na^+-concentration response of the bare Na^+ selective membrane. This membrane showed good response over a wide Na^+ concentration range. When one side of the membrane was covered by the lipid-reconstituted NaR, continuous illumination induced an increase in membrane potential, reflecting Na^+ uptake by the photolyzed NaR. The same measurements with the NaR-disabled mutant and the H^+ pump rhodopsin showed no change in membrane potential. These results negated the contribution of electrogenicity to the membrane potential due to the NaR orientation in a specific direction, and showed that this membrane only detected the change in Na^+ concentration. By using nanosecond laser pulses, two kinds of data were obtained during a single transport cycle: one was the flash-induced absorbance change in NaR in order to detect the formation and decay of structural intermediates, and the other was the flash-induced change in membrane potential, which reflects the transient Na^+ uptake and release reactions. The flash-induced absorbance change showed the acceleration of the formation of O intermediate as the Na^+ concentration increased. The flash-induced potential change showed positive change in membrane potential during a single transport cycle. Their comparison clearly indicated that Na^+ is captured and released during the formation and decay of the O intermediate, the redshifted intermediate which appears in the latter half of the transport cycle.

GENERAL INTRODUCTION

Alternating access model of the membrane transport proteins

Membrane transport proteins play crucial roles in living cells by moving various molecules across the cell membranes. These transports are accomplished through multiple steps associated with structural intermediates. Among these steps, the substrate uptake and release are the major events and involve strategic conformational changes as proposed by the alternating access model [1]. Figure 1 shows the schematic illustration of the alternating access model. During the substrate transport, the transporter is considered to alternate between an extracellular- and an intracellular-facing intermediates in which the substrate-binding site is accessible to only one side of the membrane. Thus, these intermediates should be identified and then analyzed to obtain a deeper understanding of the transport mechanisms. However, these identifications are difficult in most cases due to the necessity of measuring two aspects: One is to detect the timing of the formation and decay of respective intermediates, and the other is to detect the timing of substrate uptake and release. Here, I report a direct identification of the intermediates for the Na^+-pump rhodopsin (NaR).

Microbial rhodopsin

Rhodopsins are photoactive membrane proteins widely spread in all three domains of life [2-3]. According to the conserved residues, they are classified into two groups. One is animal rhodopsin, most of which act as photosensors like visual pigments in the eyes. The other is microbial rhodopsin found in unicellular microorganisms that performs divergent functions, such as light-driven ion pumps, light-signal transductions, light-gated ion channels, and even light-switchable enzymes (Fig 2A). Among these, ion-pump rhodopsins are the most abundant and widely distributed in the microbial world. NaR was the third discovered ion-pump rhodopsin and is considered to function in a significantly different manner from the other two ion pumps, the H^+ pump and Cl^- pump, as described below [4].

All microbial rhodopsins are composed of seven transmembrane helices and a chromophore retinal bound to a specific Lys residue via Schiff base linkage. The molecular structure of retinal is shown in Fig 2B. Upon illumination, retinal isomerizes from an all-*trans* to a 13-*cis* configuration, distorting the protein conformation. This energized intermediate state thermally relaxes to the original state through various

structural intermediates. During these cyclic reactions called photocycles, microbial rhodopsins perform their respective functions.

Unique feature of Na^+-pumping rhodopsin

In the dark states, the Schiff bases are commonly protonated. The resultant positive charges are a prerequisite for both visible light absorption and the light-induced functions themselves. These protonated Schiff bases (PSBs) are also utilized in ion pumps. For the H^+ pump, the first H^+ transfer occurs from PSB to a nearby Asp residue upon illumination [5-6]. This H^+ transfer is essential to drive the multiple subsequent H^+ transfer reactions, which finally accomplish active H^+ transport across the cell membrane. For the Cl^- pump, the substrate Cl^- binds in the vicinity of a Schiff base NH^+, which is oriented toward the extracellular (EC) side [7-8]. Upon photoinduced isomerization, the NH^+ turns toward the cytoplasmic (CP) side, which results in driving the Cl^- into the CP channel. The PSB is a prerequisite for Cl^- binding and thus essential for Cl^- pump function [9]. Different from Cl^-, cations cannot bind near the PSB due to the repulsion between the positive charges. Thus, microbial rhodopsin has been considered to be unable to pump cations (other than H^+) before the discovery of NaR [10-11]. Indeed, for the nonphotolyzed NaR, the substrate Na^+ has not been identified in the vicinity of the PSB [11-13]. Nevertheless, NaR can pump Na^+ outward.

Previous studies on NaR showed that the substrate Na^+ is transiently captured after illumination and then released before the end of the photocycle [11]. However, these uptake and release reactions have not been directly detected. Thus, their timing and the relevant intermediates have been suggested from indirect observations.

Application of Na^+-selective membrane

Here, I show direct detection of the Na^+-capture and release processes by using a Na^+-selective membrane. This Na^+-selective membrane contains the Na^+-ionophore, which has two crown ethers and can interact specifically with Na^+ that fits the pore size of the rings. By using this membrane, I detected transient Na^+ concentration changes associated with Na^+ uptake and release reactions during a single transport cycle. These timings closely match the formation and decay of O, which was detected by the flash-induced absorbance changes.

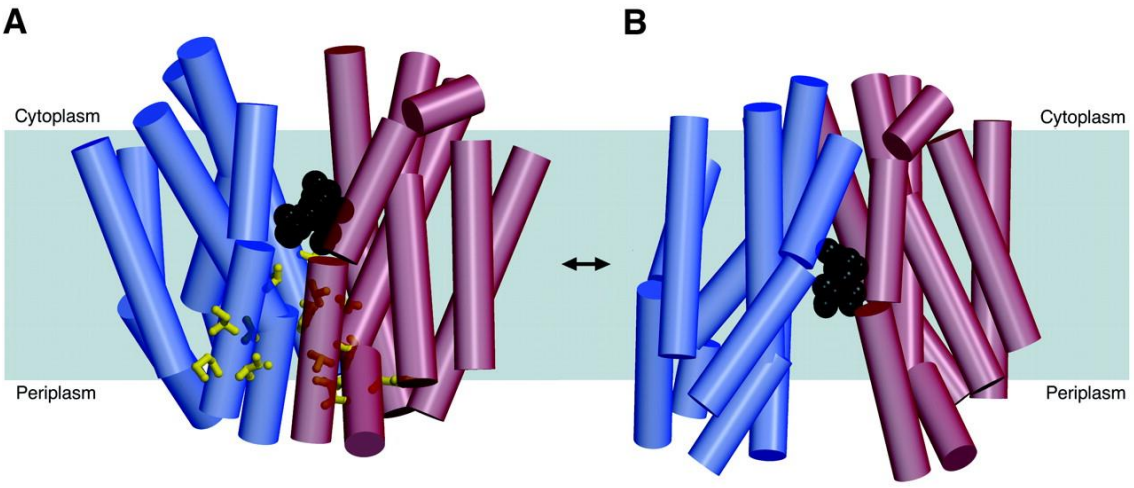

Fig 1. Schematic illustration of the alternating access model [14]. The predicted conformation changes are shown for the Lactose sympoter. (A) Inward-facing conformation determined by the X-ray structural analysis. (B) A possible model for the outward-facing conformation based on the biochemical analyses. The substrate β-D-galactopyranosyl-1-thio-β-D-galactopyranoside (TDG) is shown in black.

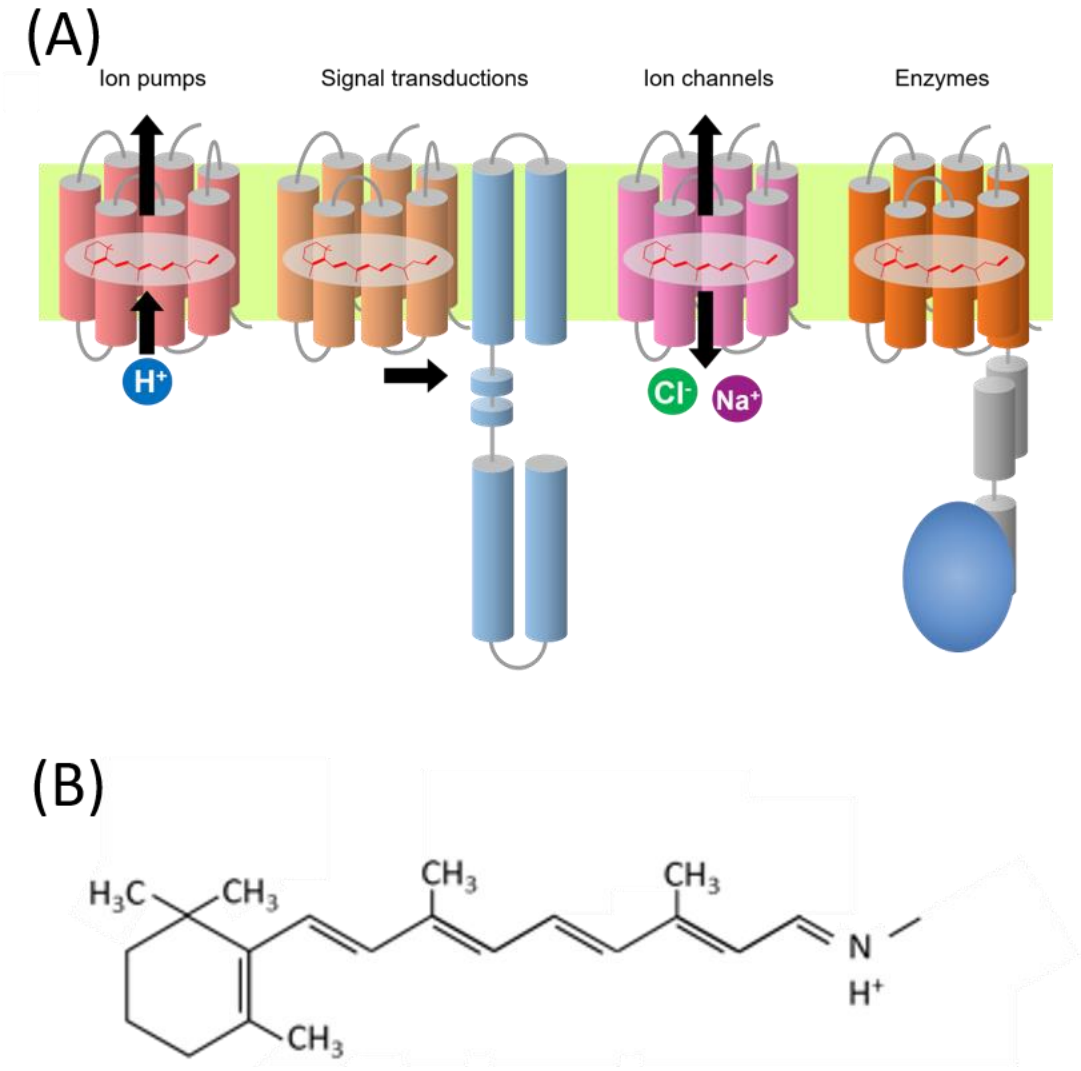

Fig 2. (A) Function of microbial rhodopsin. Microbial rhodopsin has various functions such as light-driven ion pumps, light-signal transductions, light-gated ion channels, and light-switchable enzymes. (B) The molecular structure of all-*trans* retinal.

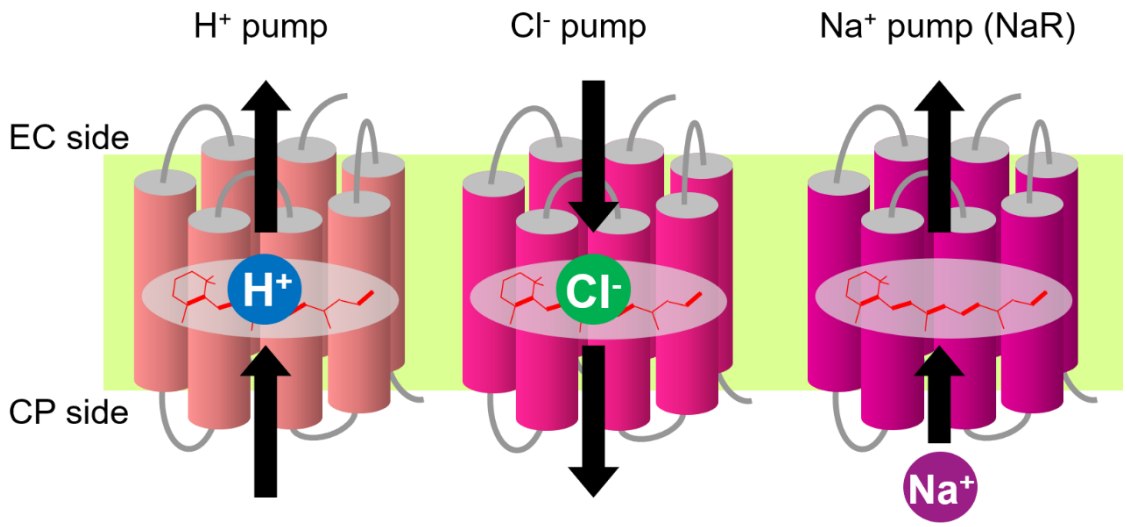

Fig. 3 The scheme of ion-pumping rhodopsins

PART I: Construction of photochemical cell equipped with the Na^+-selective membrane

INTRODUCTION

For H^+-pump rhodopsins, the timing of H^+ release and uptake have been conventionally detected by a pH indicator dye pyranine [15-17]. Pyranine rapidly induces the changes in the absorption spectrum in response to changes in pH (Fig 1-1A). So, the dye has been employed to detect the changes in the H^+ concentration by H^+ uptake and release of H^+ pumps. During a single photocycle, the H^+ pump induces a H^+ concentration change due to the time difference between H^+ release at the EC side and the H^+ uptake at the CP side. This change in H^+ concentration is ordinarily 0.1–1 μM, which is near to or larger than the dissociation constant of pyranine for H^+ (~0.05 μM) [18]. Thus, pyranine causes a detectable absorbance change in response to the H^+ release and uptake reactions. For Na^+, indicator dyes are also commercially available. However, their dissociation constants (4–200 mM) are significantly higher than that of pyranine [18] (Fig 1-1B). Thus, the detection of the Na^+ concentration change is difficult unless I can concentrate NaR to an unusually high level and can photoactivate it with high efficiency. Instead of these indicator dyes, I herein employed the Na^+-selective membrane, which is a PVC membrane involving the Na^+ ionophore (Fig 1-2 A and B). In this part, I explain the principle of the detection of changes in Na^+ concentration with Na^+-selective membrane and shows the response of a bare Na^+-selective membrane.

MATERIALS AND METHODS

Preparation of Na^+-selective membrane

The photograph of Na^+-selective membrane and the molecular structure of bis(12-crown-4) are shown in Fig 1-2A and B. A polyvinyl chloride (PVC)-based membrane was prepared using bis(12-crown-4) (Dojindo Lab, Kumamoto, Japan) and o-nitrophenyloctylether (NPOE) for the Na^+ ionophore and the plasticizer, respectively. PVC (average polymerization degree, 1050) was purchased from Wako Chemicals (Osaka, Japan) and used without further purification. The PVC (80 mg), Bis(12-crown-4) (8 mg) and NPOE (160 mg) were dissolved in tetrahydrofuran (2.4 ml). The solution was poured into a Petri dish (5.9 cm^2 in area), and the solvent was evaporated at room temperature. The resulting membrane was transparent and approximately 0.1-0.2 mm thick.

Measurements of Na^+-concentration response of bare Na^+-selective membrane

The schematic illustration of the electrochemical cell is shown in Fig. 1-2C. This cell consists of two Teflon chambers with holes (5 mm in diameter), which were the same as those described by Muneyuki et al. [19]. A disk 10 mm diameter was cut from the PVC membrane and inserted in the holes between the chambers. The "sample" chamber has another hole for the light activation experiments.

The basal buffer solution for the membrane potential measurements was 50 mM Tris-HCl, pH 8.5. Before all measurements, both chambers were filled with a buffer containing 1 M NaCl and incubated for 1 h for the conditioning of the PVC membrane. Then, the buffer solution in the sample chamber was replaced with a buffer containing the appropriate concentration of NaCl, which was made by mixing the 100 mM NaCl and 100 mM KCl buffers so that the ionic strength was kept constant. After any replacements of the buffers, the samples were left for 5 min to equilibrate. All measurements were performed at room temperature (~25 °C).

RESULTS AND DISCUSSION

Application of the Na^+-selective membrane for the Na^+- transfer reactions

When two solutions are separated with this membrane as shown in Fig. 1-2C, the partitioning of Na^+ occurs at two solution/membrane interfaces, which lead to the respective phase-boundary potentials. Within the membrane, the Na^+-ionophore complex distributes equally, and so the potential difference does not exist. As a result, the membrane potential (Ψ) is governed by the sum of two phase-boundary potentials and thus described by the Nernst equation [20]:

$$\Psi\ (\mathrm{mV}) = -59.2 \log [Na^+]/[Na^+]_{ref}\ (\text{at } 25.0\ ^{o}\mathrm{C}) \quad (1)$$

where Ψ stands for the electric potential of the sample medium with respect to that of the reference medium, and $[Na^+]$ and $[Na^+]_{ref}$ represent the Na^+ concentrations in these mediums, respectively. For the detection of Na^+ transfer reactions, I deposited the lipid-reconstituted NaR on one side of the membrane so that the illumination induces a large change in Na^+ concentration near the PVC membrane. In response to the Na^+ concentration change, the phase-boundary potential also changes at this side, which in turn causes the change of membrane potential. The change of phase-boundary potential occurs very rapidly. Thus, the membrane potential can follow the light-induced change in the Na^+ concentration.

Na^+-concentration response of the bare Na^+-selective membrane

First, I tested the response of a bare Na^+-selective membrane. In Fig. 1-3, the membrane potential is plotted against the Na^+ concentrations in the sample medium while keeping the Na^+ concentration at 1 M for the reference medium. This figure shows a slope of −50.0 mV/decade, which is close to the ideal Nernstian slope of −59.2 mV/decade. The reason for the slight difference is not known. However, the slope is almost constant over a wide Na^+ concentration range, indicating that the PVC membrane actually senses the Na^+ concentration.

(A) H^+ sensitive dye (K_d = 50 nM)

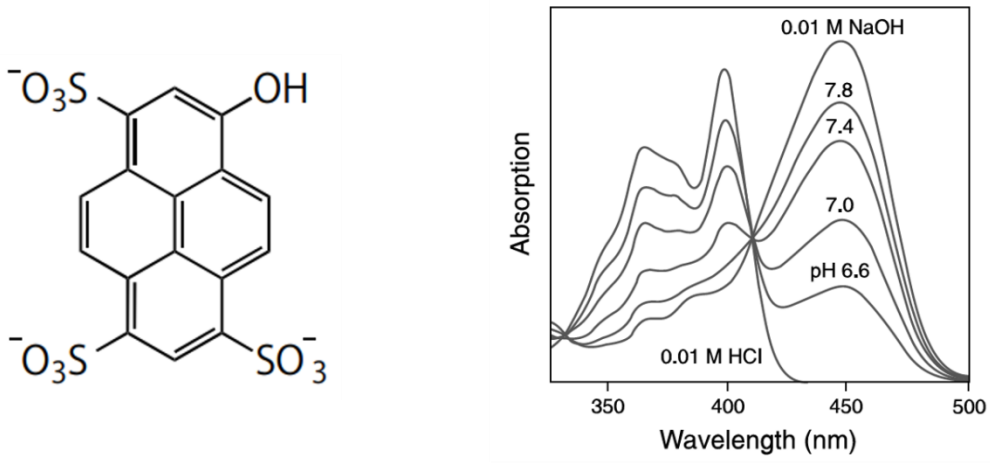

(B) Na^+ sensitive dye (K_d = 4 - 200 mM)

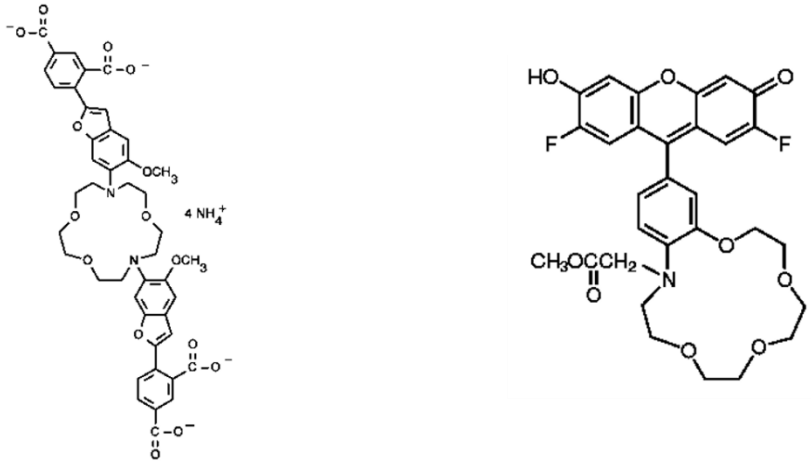

Fig 1-1. The ion sensitive dyes. (A) The molecular structure and dissociation constant of H^+ sensitive dye (pyranine) and the pH-dependent absorbance spectra of pyranine. (B) The molecular structure and dissociation constant of Na^+ sensitive dyes (left: SBFI, right: CoroNa^{TA} Green) [18].

(A) Na^+-selective membrane

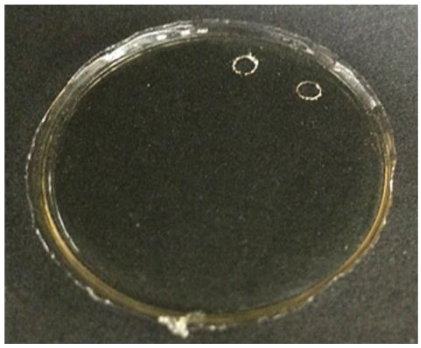

(B) Na^+ ionophore

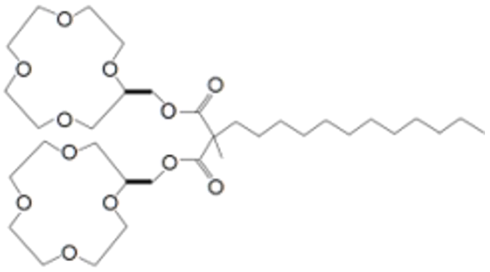

(C)

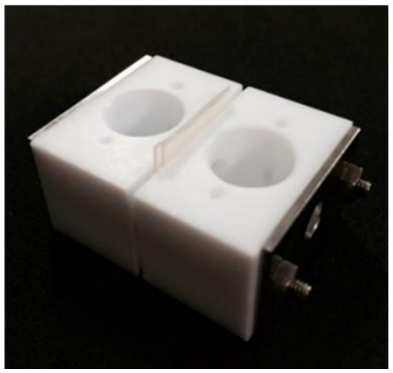

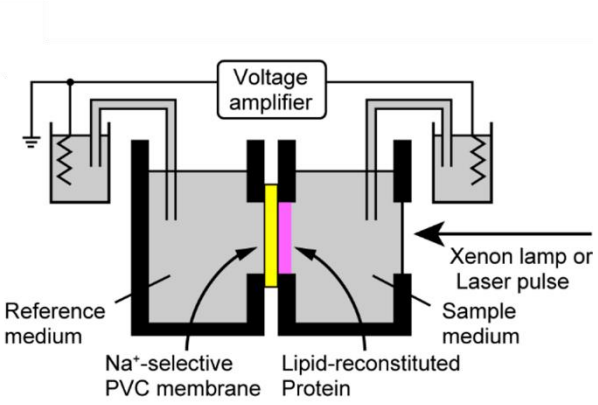

Fig1-2. (A) Photograph of Na^+-selective membrane. (B) The molecular structure of Na^+ ionophore bis(12-crown-4). (C) Photograph and schematic description of the photochemical cell used in this study.

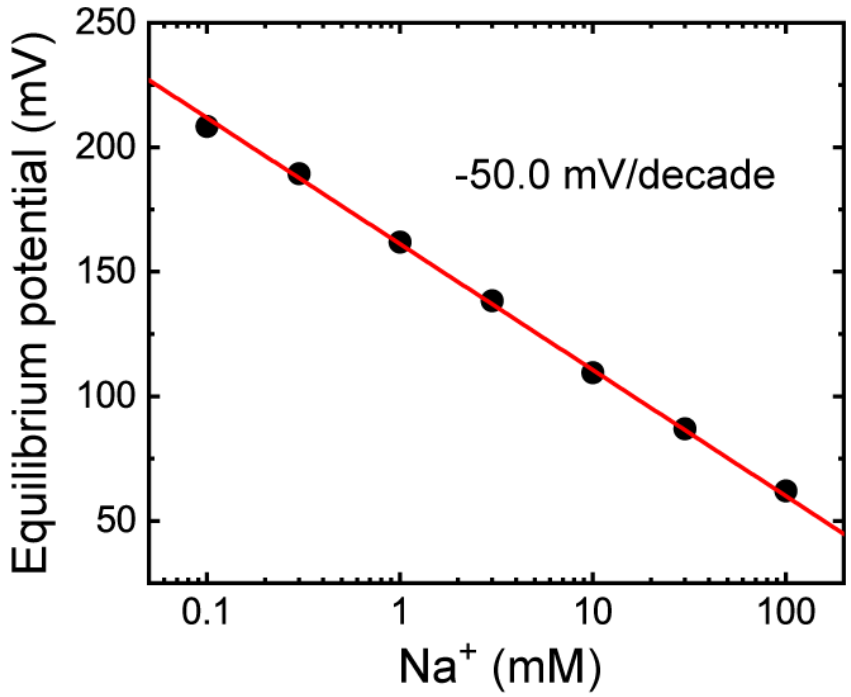

Figure 1-3. The Na^+-concentration responses of the bare Na^+-selective membrane. Reprinted with permission from {Keisuke, Murabe; Takashi, Tsukamoto; Tomoyasu, Aizawa; Makoto, Demura; Takashi, Kikukawa. Direct Detection of the Substrate Uptake and Release Reactions of the Light-Driven Sodium-Pump Rhodopsin. *J. Am. Chem. Soc.* 2020, 142, 37, 16023–16030.}. Copyright {2020} American Chemical Society.

PART II: Detection of Na^+-transfer reactions of Na^+-pumping rhodopsin

INTRODUCTION

Discrepancy in the reports about the Na^+-transfer reactions of Na^+-pumping rhodpsin

Figure 2-1 shows the typical photocycle scheme of NaR. The absorption spectroscopy is often used to observe the process of formation and decay of structural intermediates during photocycle. The flash-induced absorbance changes revealed the photocycle of NaR involving sequential intermediates that red-shifted K, blue-shifted L/M equilibrium state, red-shifted O and the subsequent intermediate (hereafter designated as NaR´). And they also revealed a faster formation of an O intermediate with a higher Na^+ concentration [11, 21-22]. This acceleration suggests the Na^+ uptake during the O formation. NaR´ has almost the same absorption spectrum as the dark state [23], suggesting that Na^+ is already absent in NaR´, at least around the retinal. Thus, Na^+ is supposed to be captured and released during the formation and decay of O. However, these assignments seem to be somewhat inconsistent with the behavior of O decay reported for a NaR from the eubacterium *Gillisia limnaea* (GLR) [14]: Similar to its formation, its O decay also becomes faster as the Na^+ concentration increases. Concerning the Na^+ uptake, a different timing was also suggested by the QM/MM study, which assigned it to the formation of earlier intermediates (K or L) but not to O formation [24]. This analysis also suggested that there are two Na^+ ion binding sites inside the protein. On the other hand, the Na^+ involvement at O has been supported by recent structural analyses, where Na^+ was identified around the PSB in the structures assigned to O [25-26]. These structures are in clear contrast to those in the nonphotolyzed states, in which Na^+ is not identified inside the protein [12-13]. In these structural analyses, NaR has only one binding site inside the protein. In this way, various studies about Na^+ transport have been conducted, but the details of the Na^+ transport mechanism of NaR remain unclear.

Na^+-pumping rhodopsin is a hybrid pump

NaR is a light-driven sodium pump that uses the energy of light to actively transport Na^+ from the cytoplasmic side to the extracellular side against a Na^+-concentration gradient. Under physiological conditions, NaR outwardly pumps Na^+. However, in the absence of Na^+, NaR pumps H^+. This indicates that NaR is a hybrid pump that has two different ion pumping cycles, which are the Na^+-pumping cycle and H^+-pumping cycle.

Fig 2-2 shows the switching of these cycles that depends on the concentration of Na^+. In the presence of high Na^+-concentration, NaR pumps Na^+. As Na^+-concentration decreases, the proportion of Na^+-pumping cycle decreases, and NaR cycle switches to the H^+-pumping cycle. Therefore, competition between Na^+ and H^+ determines the two alternative transport cycles.

MATERIALS AND METHODS

Gene preparation

Escherichia coli strain DH5α was used for DNA manipulation. Throughout this study, we used a NaR called GLR, which was mentioned above. The GLR gene (GenBank accession no. EHQ02967) with codons optimized for *E. coli* expression was chemically synthesized (Funakoshi, Tokyo, Japan) and inserted into the *Nde*I/*Xho*I site of the pET-21c vector (Merck). This plasmid results in GLR with additional amino acids in the C terminus (-LEHHHHHH). Using almost the same procedure, a proteorhodopsin (PR) gene was inserted into the pET plasmid. The PR gene sequence is identical to that in a plasmid reported previously [27]. The D116N mutation was introduced into GLR using the QuikChange site-directed mutagenesis kit (Stratagene, La Jolla, CA, USA). The DNA sequences were confirmed by a standard method using an automated DNA sequencer (Model 3100; Applied Biosystems, Foster City, CA, USA).

Protein expression, purification and the lipid reconstitution

The protein expression, purification, and the lipid reconstitution were performed as previously described [28-30]. The proteins were expressed from *E. coli* BL21(DE3) cells. The cells were grown at 37 °C in 2×YT medium supplemented with 50 μg/mL ampicillin. At the late exponential growth phase, the expression was induced by the addition of 1 mM isopropyl-β-D-thiogalactpyranoside in the presence of 10 μM all-*trans* retinal. After 3 h of induction, colored cells were harvested by centrifugation (6,400 × g, 8 min at 4 °C) and washed once with buffer (50 mM Tris-HCl, pH 8.0) containing 5 mM $MgCl_2$.

Then, the cells were broken with a French press (Ohtake, Tokyo, Japan) (100 MPa × 4 times). After removing the undisrupted cells by centrifugation (5,600 × g, 10 min at 4 °C), the supernatant was ultracentrifuged (178,000 × g, 90 min at 4 °C). The collected cell membrane fraction was suspended with the same buffer containing 300 mM NaCl and 5 mM imidazole and was then solubilized with 1.5% n-dodecyl β-D-maltopyranoside (DDM) (Dojindo Lab, Kumamoto, Japan) at 4 °C overnight. After removal of the insoluble fraction by ultracentrifugation (178,000 × g, 60 min at 4 °C), the solubilized proteins were subjected to Ni-NTA agarose (Qiagen, Hilden, Gerrmany). The unbound proteins were removed by washing the column with 10 column volumes of wash buffer (50 mM sodium phosphate, pH 7.5) containing 400 mM NaCl, 50 mM

imidazole and 0.05% DDM. The bound protein was eluted with buffer (50 mM Tris-HCl, pH 7.0) containing 300 mM NaCl, 500 mM imidazole and 0.1% DDM.

The purified proteins were mixed with a suspension of phosphatidylcholine (PC) from egg yolk (Avanti, Alabaster, AL, USA) at a protein: PC molar ratio of 1:30. After incubation for 1 h at room temperature, the detergent was removed by gentle stirring overnight (4 °C) in the presence of SM2 Adsorbent Bio-Beads (Bio-Rad, Hercules, CA, USA). The reconstituted proteins were separated from the Bio-Beads by filtration and then collected by centrifugation.

Measurement of light-induced Na^+ concentration changes

For the experiments using proteins, the assembled cell was first placed on its side so that the lipid reconstituted proteins could be deposited horizontally onto the PVC membrane. For deposition, the reconstituted proteins were suspended in distilled water with a protein concentration of 10 μM, where we assumed a molar extinction coefficient of 45,000 M^{-1} cm^{-1} at the respective λmax. The suspensions of 50 μL were applied on the surface of the PVC membrane, followed by the evaporation of water under reduced pressure to produce a dried film. This procedure was performed in duplicate. As a result, approximately 1.0 nmol of proteins were deposited on the PVC membrane. These proteins were tightly bound to the membrane, and their detachment was negligible during the following experiments.

For activation of the proteins, two light sources were used. The source for 1 s illumination was a 150 W Xenon arc lamp in combination with three glass filters (IRA-25S, KL-53 and Y-46; Toshiba, Tokyo, Japan), which provided green light with a maximum intensity at approximately 530 nm. The light duration was controlled by a mechanical shutter. The source for a 5 ns flash (532 nm, 1.2 mJ/pulse) was a second harmonic of a Q-switched Nd:YAG laser (Minilite I, Continuum, San Jose, CA, USA). In both cases, the light-induced potential changes were measured by using a homemade amplifier (response time ≈ 9 μs), which was equipped with a 0.033 Hz low cut filter for the elimination of the baseline drift. For the calculations of the light-induced potential changes, the data before illumination were adopted as baselines. To improve the S/N ratio, the signals were averaged over 10 times for 1 s illumination and 100 times for a 5 ns flash, respectively.

Measurements of flash-induced absorbance changes

The suspensions of the reconstituted proteins were activated by a 7 ns laser pulse (532 nm, 5 mJ), and the subsequent absorbance changes were recorded with a single wavelength kinetic system. The details of the apparatus are described elsewhere [31]. To improve the S/N ratio, 30 laser pulses were used at each measurement wavelength. The buffer solutions were the same as those for the membrane potential measurements. All data were obtained at 25 °C.

Measurements of ion pumping activities

The GLR activity was measured in *E. coli* suspensions using a pH electrode, which detects the pH changes by the pump activity of H^+ itself or passive H^+ transfer in response to the membrane potential created by the pump activity for another ion. The E. coli suspensions were as follows. The cell expressing GLR were harvested at 3,600 g for 5 min at 4 °C and washed twice with an unbuffered solution containing 200 mM salt (NaCl, KCl). They were resuspended in the same salt solution and gently shaken overnight as 4 °C in the presence of 10 μM carbonyl cyanide m-chlorophenyl hydrazone (CCCP). Then, the cells were washed twice with the same salt solution without CCCP and finally suspended at an A660 of 0.5. This cell density was approximately 5% of the corresponding value for the original culture medium contains at least 15 μg/mL GLR. For the activation of GLR, 530 ± 17.5 nm green LED (LXHL-LM5C, Philips Lumileds Lighting Co., San Jose, CA) was used.

RESULTS AND DISCUSSION

Na^+-concentration change due to the Na^+-transfer reactions

I examined the effect of a continuous illumination on the membrane potential. For the bare membrane, no changes were observed (data not shown). For the lipid reconstitution, I employed a high protein to lipid ratio (NaR: lipid = 1: 30). Thus, NaR was incorporated into the lipid membrane fragment, not into the spherical liposome. As a result, the light-induced change in Na^+ concentration should reflect the order of Na^+ uptake and release during the transport cycle. If the uptake occurs first followed by release, the Na^+ concentration should decrease under illumination. On the other hand, if the release occurs first followed by uptake, the Na^+ concentration should increase. As shown in Fig. 2-3, a positive potential change was observed for the membrane covered with NaR. Here, the NaR was deposited on the membrane surface facing the sample medium, indicating that the photolyzed NaR induces a decrease in Na^+ concentration. Therefore, NaR surely captures Na^+ after photoactivation. The potential change has a shape weakly differentiated, reflecting a weak low cut filter (0.033 Hz) involved in the amplifier. This differentiated shape is close to the output when we input the square wave voltage into the amplifier (Fig. 2-4). Thus, the "true" change in Na^+ concentration should also be close to the square shape. The potential changes increasing Na^+ concentration, the potential change became larger, reflecting the increase of NaR molecules undergoing the Na^+-pumping photocycle. However, the potential change began to decrease with further increases in Na^+ concentration and finally disappeared at 100 mM Na^+ (Fig. 2-3A – H). This behavior reflects that the potential change ($\Delta\Psi$) depends on not only the light-induced change in Na^+ concentration ($\Delta[Na^+]$) but also the Na^+ concentration in the bulk solution ($[Na^+]$). This relationship is theoretically described by Eq. 2,

$$\Delta\Psi\ (\mathrm{mV}) = -50.0 \log (1 + \Delta[Na^+]/[Na^+]) \quad (2)$$

where the coefficient of "−50.0" represents the slope in Fig. 1B. At a high Na^+ concentration ($[Na^+]$), the value of $\Delta[Na^+]/[Na^+]$ is almost zero, and thus the $\Delta\Psi$ becomes negligible ($\Delta\Psi = -50.0 \log (1) = 0$).

During the NaR deposition, NaR might orient in a specific direction. If this is the case, the electrogenicity might be induced under illumination and then might contribute to the potential change. However, this potential change should remain even at a high Na^+

concentration. Thus, a negligible potential change at a high Na^+ concentration (Fig. 2-3A) reflects that the PVC membrane senses only the change in Na^+ concentration. This consideration was further confirmed by using D116N NaR and the H^+ pump PR. As shown in Fig. 2-3I and J, no potential changes were observed in both cases. The D116 residue is located near PSB (Fig. 2-5A) and its replacement by Asn is known to remove the Na^+-pump activity [11]. The data for PR (Fig. 2-3J) indicates no sensitivity of the PVC membrane against the local pH change. NaR is called a "hybrid pump", because NaR pumps H^+ if the medium contains neither Na^+ nor Li^+ [11]. As shown in Fig. 2-6, this feature is also preserved in the GLR used in this study. Thus, at a lower Na^+ concentration, most GLR acts as a H^+ pump. Even in this condition, the membrane potential reflects only the change in Na^+ concentration evoked by the GLR undergoing a Na^+-pump cycle.

Many microbial rhodopsins are known to adopt oligomeric states in the cell membranes. Concerning the lipid-reconstituted NaR, the high-speed AFM imaging proved its pentameric state [32], whose assembly was essentially the same with that observed in the crystal structure [13]. Thus, NaR used in this study probably takes pentameric state.

I explain the reason that I selected GLR as the measurement sample. At the start of my study, GLR was known as NaR that transports only Na^+ during photocycle, and showed high affinity Na^+-binding site [21], so I employed GLR as the sample that conform to measurable Na^+ concentration ranges of Na^+-selective membrane.

Intermediates associated with the Na^+ uptake and release reactions

For the identification of the intermediates, two kinds of data were obtained using nanosecond laser pulses: One is the flash-induced transient absorbance change, and the other is the flash-induced membrane potential change. Figure 2-7A, B, and C show the flash-induced absorbance changes measured at typical three wavelengths. Here, eight traces with 0 – 30 mM Na^+ are plotted simultaneously. Due to the fast decay, the earliest intermediate K was not observed by our apparatus. Instead, the blue-shifted intermediates, which were previously assigned to L and the subsequent M, were first observed at 410 nm (Fig. 2-7A). With concomitant decay of their equilibrium, the redshifted O appears at 590 nm (Fig. 2-7B). Another absorbance change at 510 nm reflects the depletion and recovery of the dark state through the last intermediate NaR´ (Fig. 2-7C). This photocycle scheme is summarized in Fig. 2-1. As described above, O has been considered to involve Na^+ inside the protein. By elevating the Na^+

concentration, the accumulation of O becomes prominent, and the peak position shifts to an earlier time (Fig. 2-7B). Thus, the next concern is whether the changes in membrane potential match with the accumulation of O at any Na^+ concentration in terms of both amplitude and timing.

As shown in Fig.2-7B, even at 0 mM Na^+, the O-like intermediate appears at 590 nm. This "pseudo" O is the intermediate appearing in the H^+ pumping cycle. As the Na^+ concentration increases, the contribution of another O, which appears in the Na^+-pumping cycle, becomes dominant. For the comparison with the membrane potential signals, I removed the contributions of the "pseudo" O from the measured absorbance changes as described below. Compared to the "pseudo" O, the other O has a faster decay rate. Thus, the positive absorbance changes in the late time region (> 1 c) reflect only the accumulations of the "pseudo" O. In Fig. 6E, the absorbance changes at 2 s (ΔA_{590}, 2 s) are plotted against the Na^+ concentration. Here, the smooth line is the best fitting result with the equation:

$$\Delta A_{590,\,2\,s} = \Delta A_0 \times f_{O\text{-like}} = \Delta A_0 / (1 + [Na^+]^n / K_{0.5}{}^n) \quad (3)$$

where ΔA_0 and n represent the $\Delta A_{590,\,2\,s}$ at 0 mM Na^+ and Hill coefficient, and $K_{0.5}$ stands for the Na^+ concentration at which the photocycle branching is at its midpoint, respectively. These determined values are ΔA_0 = 3.24 mABS, n = 0.78 and $K_{0.5}$ = 0.32 mM. In Eq. 3, f_O-like represents the mole fraction of "pseudo" O. By using the f_O-like values, the absorbance changes reflecting only O ($\Delta A_{590,\,O}$ (t)) were estimated by:

$$\Delta A_{590,\,O}(t) = \Delta A_{590}(t) - f_{O\text{-like}} \times \Delta A_{590,\,0\,mM}(t) \quad (4)$$

where ΔA_{590} (t) and $\Delta A_{590,\,0\,mM}$ (t) represent the raw data at 590 nm measured at the corresponding Na^+ concentration and at 0 mM Na^+, respectively. The calculated $\Delta A_{590,\,O}$ (t) are plotted in Fig. 2-7D.

Previously, Balashov et al. also determined the $K_{0.5}$ value for GLR with similar procedure [21]. Their determined value is 60 μM and thus significantly lower than my value (0.32 mM). This difference might originate from the different buffer conditions. They varied Na^+ concentration without the ionic strength adjustment. On the other hand, I kept the ionic strength at the constant value equivalent to 100 mM NaCl by adding the KCl salt. Indeed, when I did not add KCl salt, the $K_{0.5}$ value became very small ~90 μM (data not shown). Thus, the ionic strength and/or K^+ ion might affect the Na^+ concentration for the photocycle branching.

Figure 2-8A shows the flash-induced potential changes in the Na^+-selective membrane covered by wild-type NaR. At approximately 10–100 ms, relatively large peaks appeared. As shown in Fig. 2-7D, O accumulation also reaches its maximum in the same time region. Thus, Na^+ is probably involved at O. As the Na^+ concentration increases, the peak magnitude first increased and then decreased. Finally, the peak disappeared at 100 mM Na^+, indicating that this potential change surely originates from the Na^+ concentration change. In Fig. 2-8A, another small peak also appeared at approximately 0.1 msec. At any Na^+ concentration, this peak appeared with the same shape and the same amplitude. Similar peaks were also observed for D116N NaR and PR (Fig. 2-8B and C). Thus, these peaks are not associated with the Na^+-pumping reaction. Microbial rhodopsins and visual rhodopsin are known to show light-induced charge displacements by only their conformational changes, even though these conformational changes do not involve ion transfer reactions [33]. These simple charge displacements might induce potential changes of the PVC membrane, if the proteins are oriented in a specific direction. This type of potential change should remain even at high Na^+ concentration as similar to the peaks at approximately 0.1 ms. However, if the NaR is indeed oriented, the latter peak at 10-100 ms should also remain due to its electrogenicity, because the latter peak surely originates from the Na^+-transfer reactions. Thus, at present, the origin of the first peak is not known. Although this uncertainty, the first peak does not relate with the Na^+ uptake and release reactions. Thus, I subtracted the first peak from the potential change for the comparison with the flash-induced absorbance change. The calculated potential changes (designated as $\Delta\Psi_{Na^+}$) are shown in Fig. 2-8D, where the potential change at 100 mM Na^+ was subtracted from the potential changes at other Na^+ concentrations.

If O is the intermediate involving Na^+ inside the protein, its amount of accumulation should be proportional to the decreased Na+ concentration ($\Delta[Na^+]$). Thus, I compared these values in Fig. 7E. The filled circles represent the maximum absorbance changes in Fig. 2-7D ($\Delta A_{590,O,max}$), which indicate the maximum accumulations of O at respective Na^+ concentrations. The open circles represent the magnitude of the maximum decreases of Na^+ concentration ($-\Delta[Na^+]_{max}$), which was calculated by the following equation:

$$\Delta[Na^+]_{max} = [Na^+]\cdot (10^{-\Delta\Psi max/50.0} - 1) \quad (5)$$

This equation was derived from Eq. 2 and the $\Delta\Psi_{max}$ represents the maximum potential changes of $\Delta\Psi_{Na^+}$ (Fig. 2-8D) at respective Na^+ concentration. As shown in Fig.

2-8E, these two values show almost the same Na^+ dependency, indicating that O surely contains Na^+ inside the protein.

Next, I compared the time courses of O accumulation and the Na^+ concentration change. Each panel in Fig. 2-9 contains two time traces: They are the absorption changes in Fig. 2-7D ($\Delta A_{590,O}$) and the membrane potential changes in Fig. 2-8D ($\Delta\Psi_{Na^+}$), respectively. As shown here, two traces overlapped well in all panels, even though the peak positions gradually shifted depending on the Na^+ concentration. These results also emphasized that Na^+ is captured and released during the formation and decay of the O intermediate.

At low Na^+ concentrations (0.1 – 1 mM), two traces in Fig. 2-9 do not perfectly match, where the Na^+ uptakes (red traces) are slower than the formations of O (black traces). These differences might be caused by the contaminations of "pseudo" O in the black traces. As shown in Fig. 2-7B, the raw data of ΔA_{590} (t) at 0 mM, which involves only the "pseudo" O, has two peaks around 1-10 and 10-100 ms, respectively. On the other hand, at lower Na^+ concentrations, the black traces in Fig. 2-9 have shoulders around 1-10 ms, which is similar to the first peak of "pseudo" O. For the calculations of the black traces, I assumed that the time course of "pseudo" O does not change even varying the concentrations of Na^+ and/or K^+. This assumption might not be correct. If the magnitude of the first peak is altered, this peak is not completely removed by the subtraction. The remaining peaks might form the shoulders at lower Na^+ concentrations and then apparently enlarge the differences from the red traces.

Na^+ uptake reactions

As mentioned above, D116N NaR completely loses its Na^+-pumping activity [11]. This Asp residue is a counter ion of the PSB (Fig. 2-5A) and acts as a H^+ acceptor from the PSB. The resultant loss of the positive charge is considered to be essential for Na^+ passage over the Schiff base region and to allow the arrival of Na^+ at the putative binding site between N112 and D251 (Fig. 2-5A) [4, 26, 34]. In addition to this gating role, the D116 residue is also considered to directly interact with Na^+ before the movement over the Schiff base region [24-25]. Thus, this residue seems to be crucial for Na^+ binding inside the protein. My observation in Fig. 2-3I and 2-8B proved this hypothesis. As shown here, no potential change was observed for D116N NaR, indicating that this mutant even lacks the Na^+ uptake ability. The D116 residue is located deep inside the protein and is approximately 18 Å away from the protein surface (Fig. 2-5A). Despite this long distance, the Na^+ seems to come around D116 by a single

step movement during the O formation. The pathway in the CP channel should be narrow and highly hydrophobic [12-13]. Thus, NaR seems to have a mechanism to facilitate the Na^+ movement. One possibility is a transient hydration of the CP channel. Significant hydrations were indeed reported for other ion pump rhodopsins [35-37].

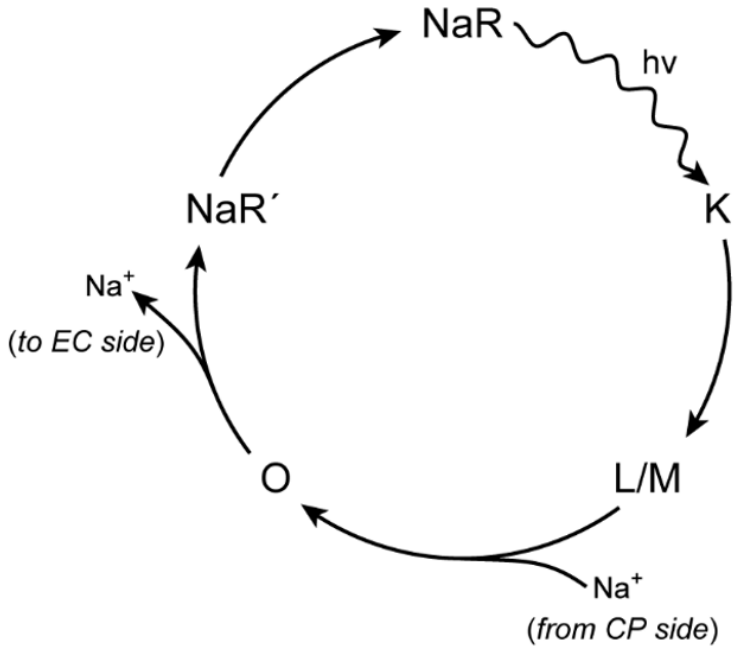

Fig 2-1. The photocycle scheme of NaR. This panel shows a typical photocycle scheme, where also indicates the timings of Na^+ uptake and release that determined in this study. L/M denotes the equilibrium of L and M intermediates. Reprinted with permission from {Keisuke, Murabe; Takashi, Tsukamoto; Tomoyasu, Aizawa; Makoto, Demura; Takashi, Kikukawa. Direct Detection of the Substrate Uptake and Release Reactions of the Light-Driven Sodium-Pump Rhodopsin. *J. Am. Chem. Soc.* 2020, 142, 37, 16023–16030.}. Copyright {2020} American Chemical Society.

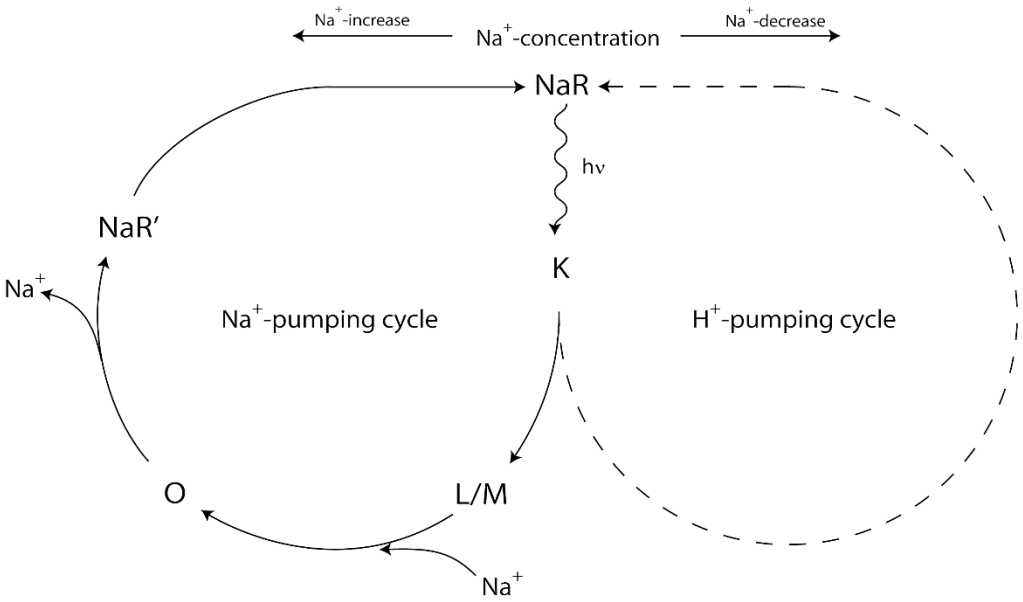

Fig 2-2. The switching of the Na^+/H^+ transport cycles. In the presence of Na^+, NaR pumps Na^+. As the Na^+-concentration decreases, the proportion of Na^+-pumping cycle decreases and cycle switches to the H^+-pumping cycle.

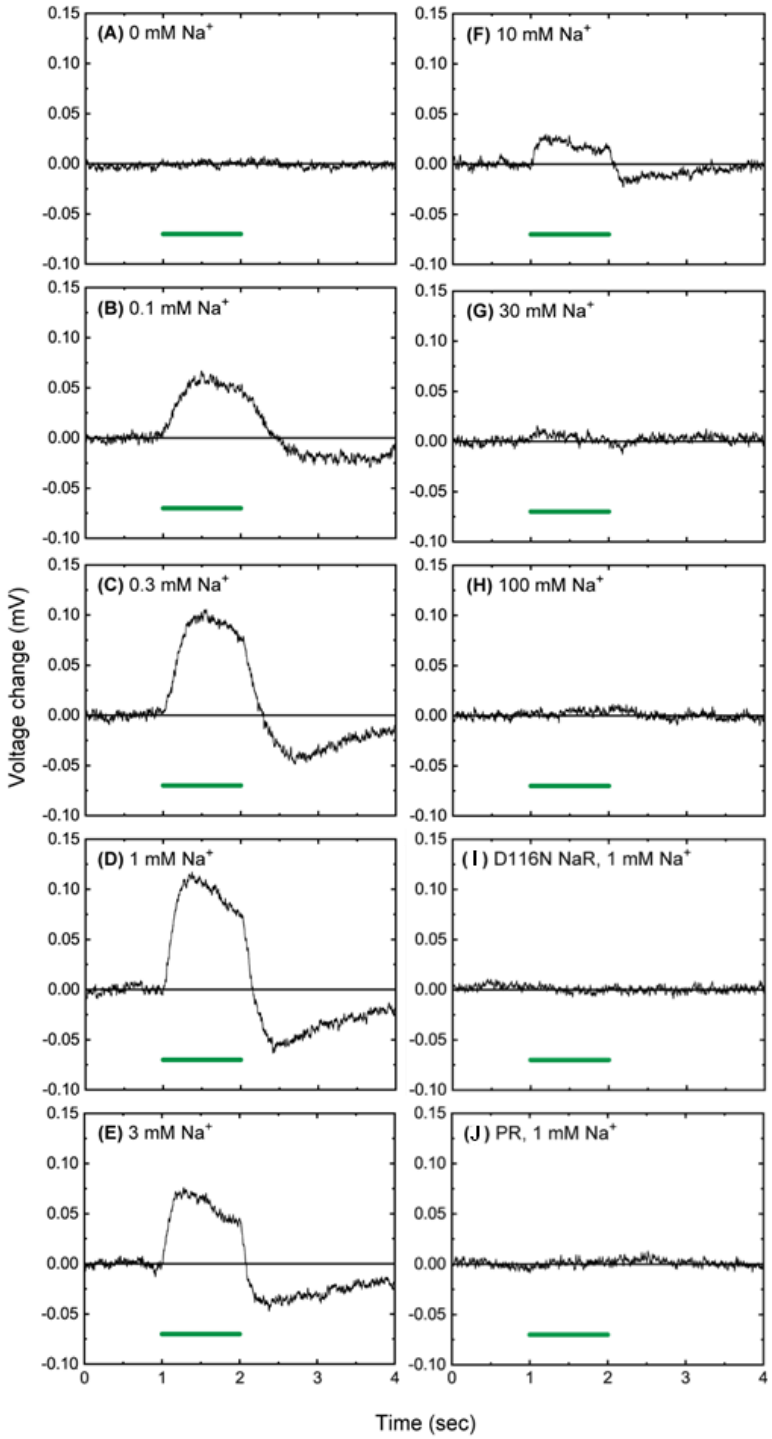

Figure 2-3. Light-induced potential change of Na^+-selective membrane at various Na^+ concentrations under continuous illumination. The membrane surfaces were covered with the lipid reconstituted NaR (A – H), its D116N mutant (I), and PR (J), respectively. The green bar indicates the period of illumination and the Na^+ concentrations in the sample mediums are indicated in the panels.

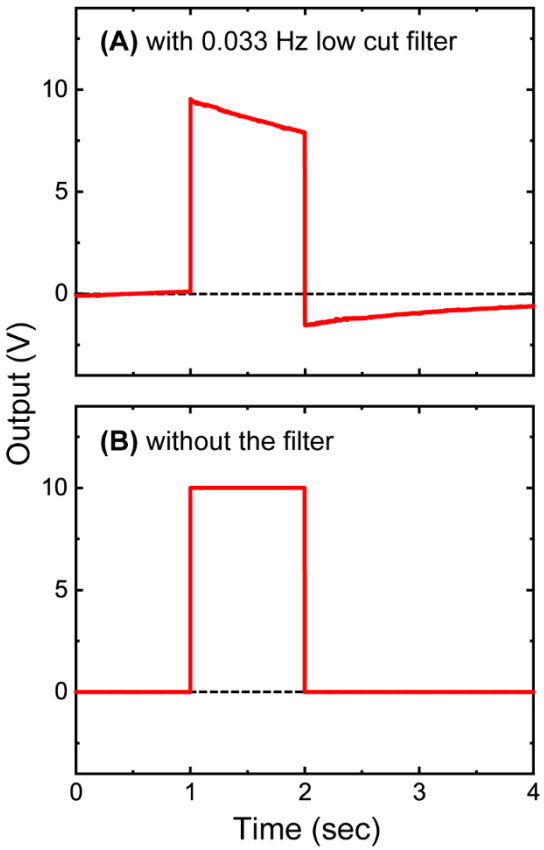

Figure 2-4. The response of the voltage amplifier for the input of square wave voltage. This amplifier is equipped with a removal 0.033 Hz low cut filter. Panels A and B show the output voltages with and without the filter, respectively. Here, we inputted the square wave voltage. The output with the filter was slightly differentiated. Reprinted with permission from {Keisuke, Murabe; Takashi, Tsukamoto; Tomoyasu, Aizawa; Makoto, Demura; Takashi, Kikukawa. Direct Detection of the Substrate Uptake and Release Reactions of the Light-Driven Sodium-Pump Rhodopsin. *J. Am. Chem. Soc.* 2020, 142, 37, 16023–16030.}. Copyright {2020} American Chemical Society.

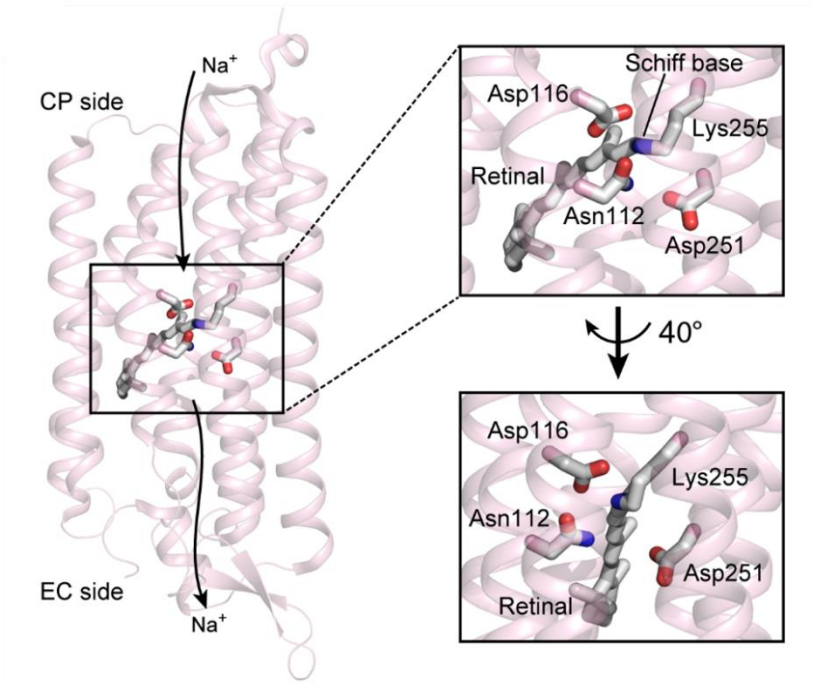

Figure 2-5. Positions of key residues for putative Na^+ binding sites. In this panel, crystal structure of NaR from *Krokinobacter eikastus* (PDB code: 3X3C) is shown with retinal and the nearby amino acid residues. Reprinted with permission from {Keisuke, Murabe; Takashi, Tsukamoto; Tomoyasu, Aizawa; Makoto, Demura; Takashi, Kikukawa. Direct Detection of the Substrate Uptake and Release Reactions of the Light-Driven Sodium-Pump Rhodopsin. *J. Am. Chem. Soc.* 2020, 142, 37, 16023–16030.}. Copyright {2020} American Chemical Society.

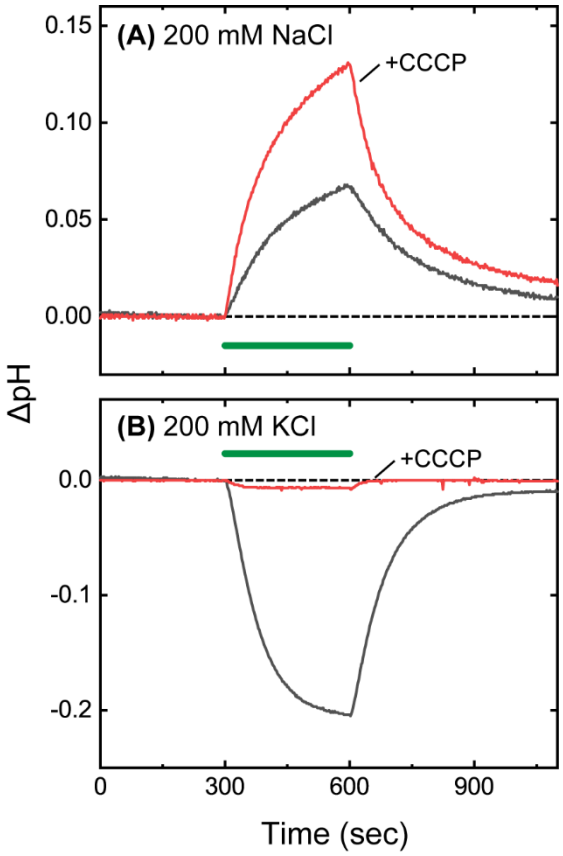

Figure 2-6. Light-induced pH changes of suspensions of *E. coli* cells expressing GLR. After harvest, the cells were starved in 200 mM NaCl or KCl overnight, respectively. These cells were washed again with the same salt solutions and then suspended so that the OD values at 660 nm became 0.5. The green bar indicates the period of green light illumination. In the presence of Na^+ (Panel A), pH increase was observed, indicating the outward Na^+ pumping activity of GLR. This activity creates inside negative potential, which drives H^+ influx and then induces pH increase. By the presence of 10 μM CCCP, the pH increase became large, reflecting the facilitation of membrane penetration of H^+. On the other hand, in the absence of Na^+ (Panel B), pH decrease was observed due to the outward H^+ pumping activity of GLR. This pH change was disappeared by the addition of 10 μM CCCP, indicating that H^+ was indeed pumped by GLR. Reprinted with permission from {Keisuke, Murabe; Takashi, Tsukamoto; Tomoyasu, Aizawa; Makoto, Demura; Takashi, Kikukawa. Direct Detection of the Substrate Uptake and Release Reactions of the Light-Driven Sodium-Pump Rhodopsin. *J. Am. Chem. Soc.* 2020, 142, 37, 16023–16030.}. Copyright {2020} American Chemical Society.

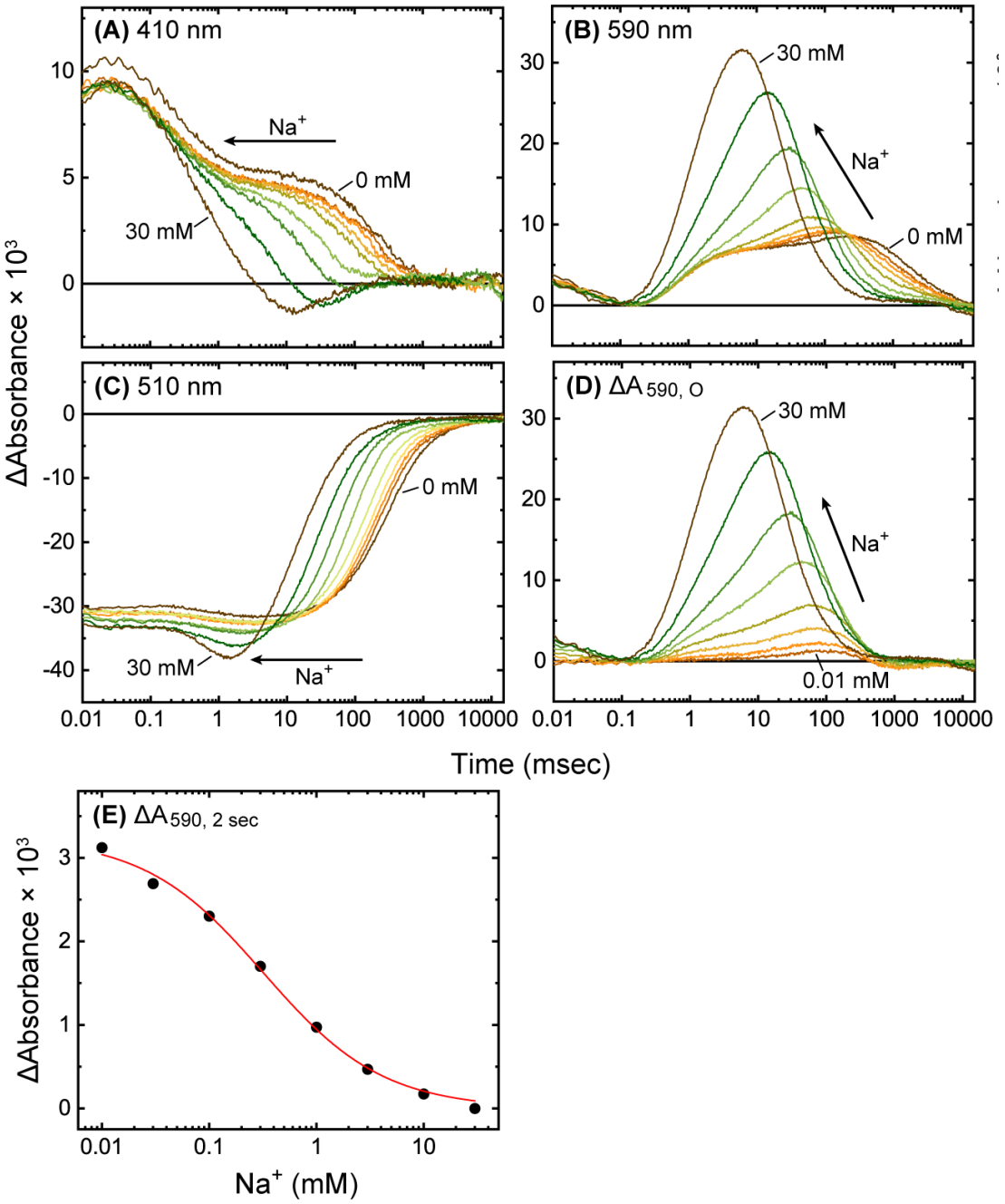

Figure 2-7. Flash-induced absorbance changes of NaR. In Panels A-C, the time-dependent changes at the typical three wavelengths are plotted. The Na+ concentrations are 0, 0.01, 0.03, 0.1, 0.3, 1, 3, 10, and 30 mM, respectively. Panel D shows the calculated absorbance changes reflecting only the accumulation of O in the Na^+-pumping cycle. These calculations used the fitting results in Panel E, where the absorbance changes at 2 s in Panel B were plotted against Na^+ concentration. The smooth line is the best fitted result with Eq. 3. For details, see the text

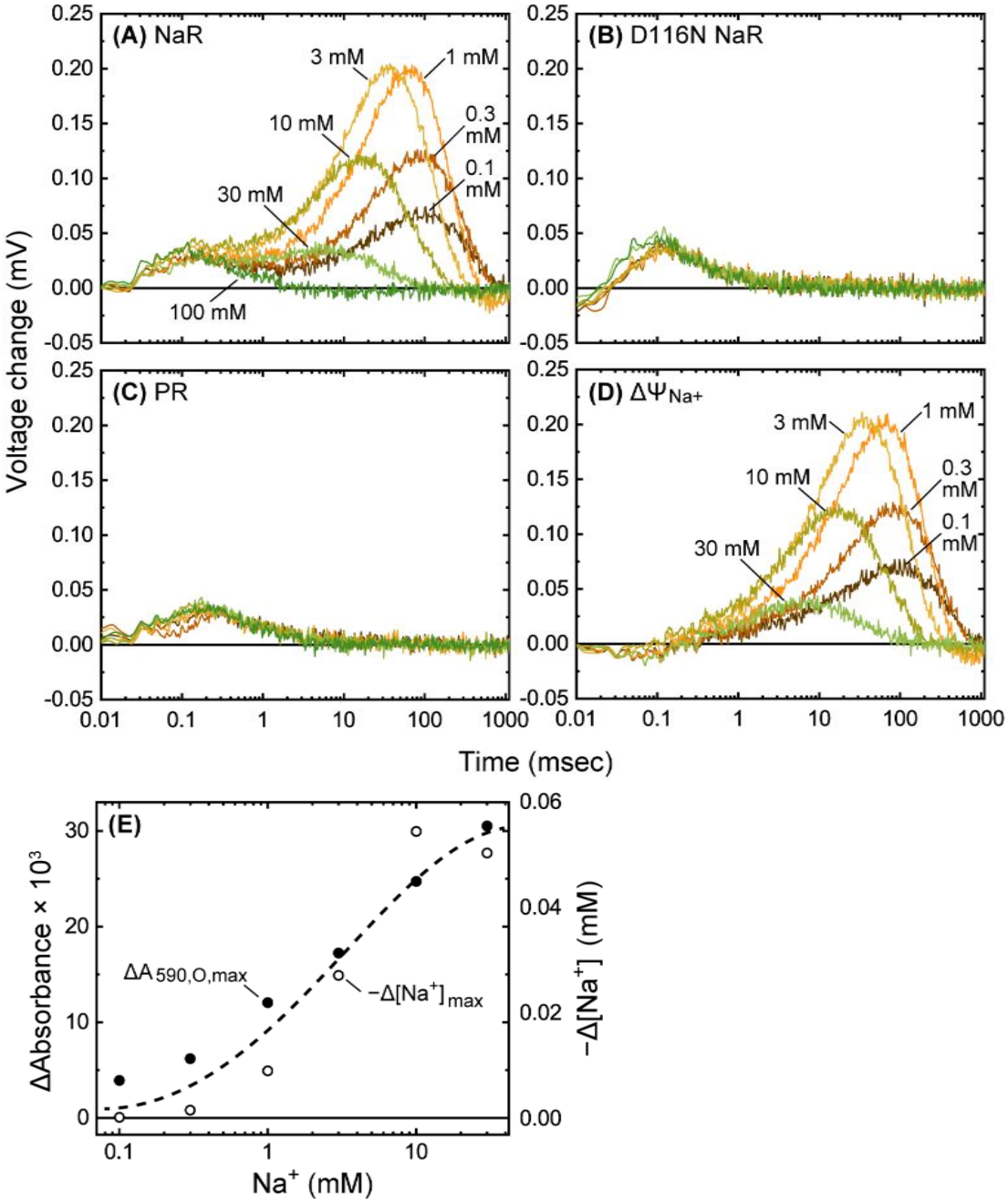

Figure 2-8. Flash-induced potential changes of the Na^+-selective membrane. The membrane surfaces were covered with the lipid-reconstituted NaR (A), its D116N mutant (B), and PR (C), respectively. Panel D shows the remaining potential changes for wild-type NaR after subtraction of trace at 100 mM Na^+. The peak values in this panel were picked up and then used for the calculations of the corresponding Na^+-concentration changes ($\Delta [Na^+]_{max}$). The calculated values were plotted in Panel E (open circles) together with the peak values of the traces in Fig. 3D ($\Delta A_{590,O,max}$, filled circles). For details, see the text.

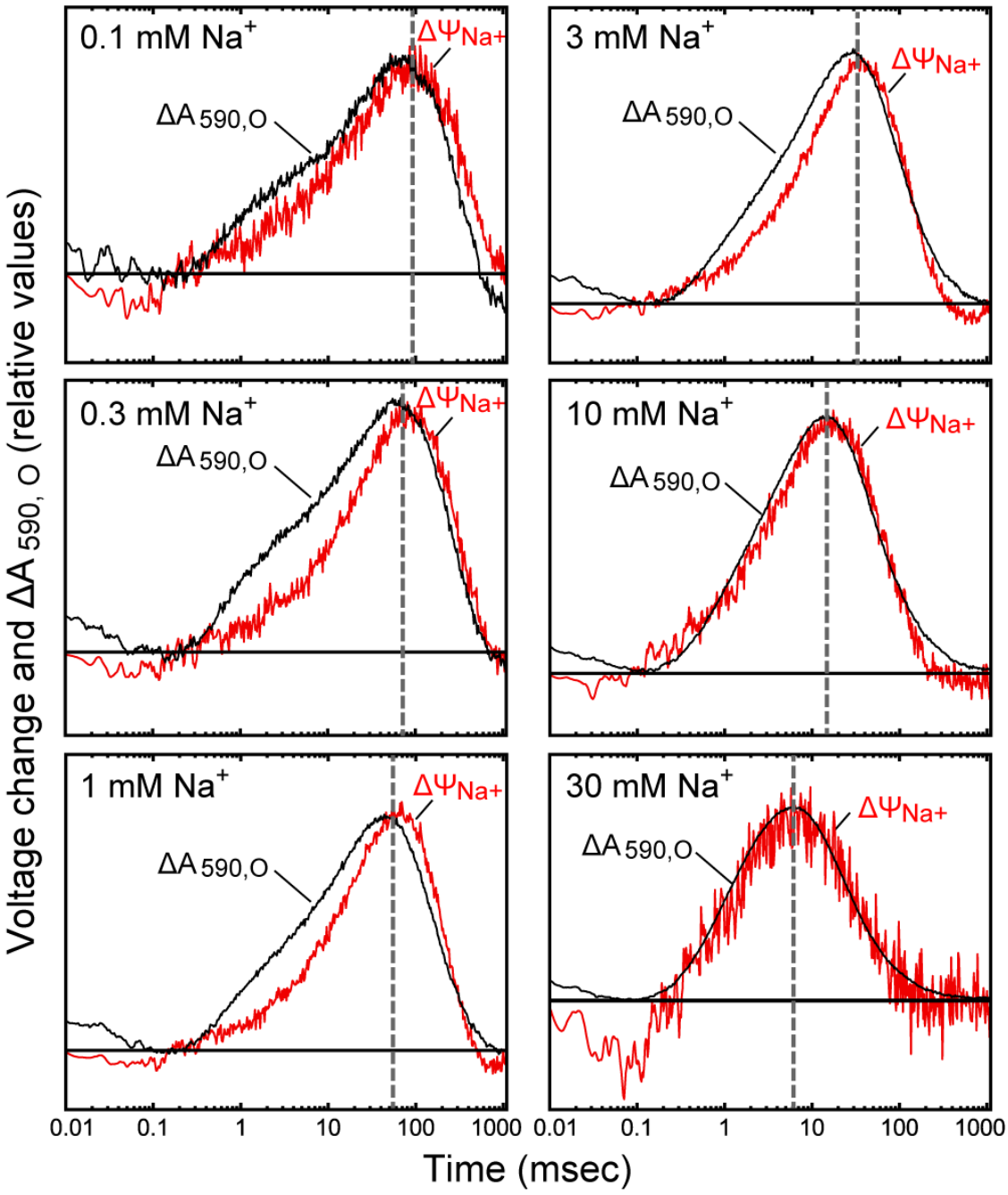

Figure 2-9. Comparisons of time courses of O accumulations and Na^+ concentration changes. The traces in Fig. 2-7D and Fig. 2-8D were plotted together with the adjusted y-axis. The two traces show almost the same time course at all Na^+ concentrations. The vertical broken lines indicate the peak positions for the clarity of their time shifts depending on the Na^+ concentration.

CONCLUSIONS

The main events of Membrane transporters are substrate uptake and release reactions during these transport cycles. This transport is accompanied with the strategic structural changes as proposed by the alternating access model. During these events, the transporter is considered to alternate between an extracellular- and an intracellular-facing intermediate in which the substrate-binding site is accessible to only one side of the membrane. Thus, these intermediates should be identified and then analyzed to obtain a deeper understanding of the transport mechanisms. However, in order to identify the intermediate, it is necessary to detect both the timing of the uptake and release of the substrate and the timing of the formation and decay of the intermediate. These detections are difficult in most cases. In this study, I report a direct identification of the intermediates for the Na^+- pump rhodopsin (NaR) with a Na^+-selective membrane. This membrane contains a Na^+ ionophore, which specifically interacts with Na^+, and can rapidly detect small changes in Na^+ concentrations. Firstly, I confirmed that a Na^+-selective membrane showed a good response of Na^+ concentration over a wide Na^+ concentration range. On this membrane, the lipid-reconstituted NaR was dried under reduced pressure. Under continuous illumination, this bared membrane did not show any potential change. But, the membrane with NaR showed the potential upshift, indicating the decrease of Na^+ concentration. When employing H^+-pump proteorhodopsin and a disabled GLR mutant, no potential shift was observed. Thus, NaR captures Na^+ after starting the photoreaction. Next, I detected flash-induced Na^+ concentration changes associated with the uptake and release reactions of NaR during its single transport cycle. The detected changes in Na^+ concentration closely matched with the O intermediate accumulations in terms of both amplitude and timing. Thus, I proved that Na^+ is captured and released during the formation and decay of O.

As mentioned above, the transporters should assume different conformations for substrate uptake and the release. Thus, there seems to exist at least two O intermediates. We previously reported that the Na^+-pumping cycle contains two subsequent redshifted intermediates and named them O1 and O2, respectively [16]. Thus, detailed characterizations of these intermediates should be performed in future investigation. Here, I employed an ion-selective membrane for the identification of the intermediate associated with the ion uptake and release reactions. This membrane is also a powerful tool for further analyses of ion transporters because I can probe the roles of individual amino acids in more detail. For example, if I find a mutant preserving the ion uptake

ability but lacking the ion transport activity, the mutated residue clearly plays an essential role in a process after the ion uptake. For NaR, analyses using various mutants are currently underway in my laboratory. Additionally, this membrane is also expected to the application to the functional analysis of membrane transport rhodopsin that transports ions other than Na^+. Since this membrane interacts with specific ions using the ionophore, it may be possible to detect changes in the concentration of other ions by changing the ionophore, while it is necessary to consider the composition of the membrane according to each ionophore. The analyses with other ion selective membrane are also currently underway in my laboratory.

REFERENCES

[1] Jardetzky, O., Simple allosteric model for membrane pumps. *Nature* **1966,** *211* (5052), 969-970.

[2] Ernst, O. P.; Lodowski, D. T.; Elstner, M.; Hegemann, P.; Brown, L. S.; Kandori, H., Microbial and animal rhodopsins: structures, functions, and molecular mechanisms. *Chem. Rev.* **2014,** *114* (1), 126-163.

[3] Spudich, J. L.; Sineshchekov, O. A.; Govorunova, E. G., Mechanism divergence in microbial rhodopsins. *Biochim. Biophys. Acta Bioenerg.* **2014,** *1837* (5), 546-552.

[4] Kandori, H.; Inoue, K.; Tsunoda, S. P., Light-Driven Sodium-Pumping Rhodopsin: A New Concept of Active Transport. *Chem. Rev.* **2018,** *118* (21), 10646-10658.

[5] Balashov, S. P., Protonation reactions and their coupling in bacteriorhodopsin. *Biochim. Biophys. Acta* **2000,** *1460* (1), 75-94.

[6] Lanyi, J. K., Bacteriorhodopsin. *Annu. Rev. Physiol.* **2004,** *66*, 665-688.

[7] Kolbe, M.; Besir, H.; Essen, L. O.; Oesterhelt, D., Structure of the light-driven chloride pump halorhodopsin at 1.8 Å resolution. *Science* **2000,** *288* (5470), 1390-1396.

[8] Kouyama, T.; Kanada, S.; Takeguchi, Y.; Narusawa, A.; Murakami, M.; Ihara, K., Crystal structure of the light-driven chloride pump halorhodopsin from *Natronomonas pharaonis*. *J. Mol. Biol.* **2010,** *396* (3), 564-579.

[9] Hayashi, S.; Tamogami, J.; Kikukawa, T.; Okamoto, H.; Shimono, K.; Miyauchi, S.; Demura, M.; Nara, T.; Kamo, N., Thermodynamic parameters of anion binding to halorhodopsin from *Natronomonas pharaonis* by isothermal titration calorimetry. *Biophys. Chem.* **2013,** *172*, 61-67.

[10] Jung, K. H. In *New type of cation pumping microbial rhodopsins in marine bacteria*, 244th ACS National Meeting & Exposition, Philadelphia, PA, August 19-23, 2012, Abstract 271.

[11] Inoue, K.; Ono, H.; Abe-Yoshizumi, R.; Yoshizawa, S.; Ito, H.; Kogure, K.; Kandori, H., A light-driven sodium ion pump in marine bacteria. *Nat. Commun.* **2013,** *4*, 1678.

[12] Kato, H. E.; Inoue, K.; Abe-Yoshizumi, R.; Kato, Y.; Ono, H.; Konno, M.; Hososhima, S.; Ishizuka, T.; Hoque, M. R.; Kunitomo, H.; Ito, J.; Yoshizawa, S.; Yamashita, K.; Takemoto, M.; Nishizawa, T.; Taniguchi, R.; Kogure, K.; Maturana, A. D.; Iino, Y.; Yawo, H.; Ishitani, R.; Kandori, H.; Nureki, O., Structural basis for Na^+ transport mechanism by a light-driven Na^+ pump. *Nature* **2015,** *521* (7550),

48-53.

[13] Gushchin, I.; Shevchenko, V.; Polovinkin, V.; Kovalev, K.; Alekseev, A.; Round, E.; Borshchevskiy, V.; Balandin, T., Crystal structure of a light-driven sodium pump. *Nat. Struct. Mol. Biol.* **2015,** *22*, 390-395.

[14] Jeff Abramson, Irina Smirnova, Vladimir Kasho, Gillian Verner, H. Ronald Kaback, So Iwata., Structure and Mechanism of the Lactose Permease of *Escherichia coli*. *Science* **2003,** *301*, 5633, 610-615.

[15] Heberle, J., Proton transfer reactions across bacteriorhodopsin and along the membrane. *Biochim. Biophys. Acta* **2000,** *1458* (1), 135-147.

[16] Kikukawa, T.; Shimono, K.; Tamogami, J.; Miyauchi, S.; Kim, S. Y.; Kimura-Someya, T.; Shirouzu, M.; Jung, K. H.; Yokoyama, S.; Kamo, N., Photochemistry of *Acetabularia* rhodopsin II from a marine plant, *Acetabularia acetabulum*. *Biochemistry* **2011,** *50* (41), 8888-8898.

[17] Iizuka, A.; Kajimoto, K.; Fujisawa, T.; Tsukamoto, T.; Aizawa, T.; Kamo, N.; Jung, K. H.; Unno, M.; Demura, M.; Kikukawa, T., Functional importance of the oligomer formation of the cyanobacterial H^+ pump *Gloeobacter* rhodopsin. *Sci. Rep.* **2019,** *9* (1), 10711.

[18] Muneyuki, E.; Okuno, D.; Yoshida, M.; Ikai, A.; Arakawa, H., A new system for the measurement of electrogenicity produced by ion pumps using a thin polymer film: examination of wild type bacteriorhodopsin and the D96N mutant over a wide pH range. *FEBS Lett.* **1998,** *427* (1), 109-114.

[19] Haugland, R. P., *The molecular probes handbook: A guide to fluorescent probes and labeling technologies*. 11th ed.; Life Technologies Corp.: Carlsbad, CA: 2010.

[20] Bakker, E.; Bühlmann, P.; Pretsch, E., The phase-boundary potential model. *Talanta* **2004,** *63* (1), 3-20.

[21] Balashov, S. P.; Imasheva, E. S.; Dioumaev, A. K.; Wang, J. M.; Jung, K. H.; Lanyi, J. K., Light-Driven Na^+ Pump from *Gillisia limnaea*: A High-Affinity Na^+ Binding Site Is Formed Transiently in the Photocycle. *Biochemistry* **2014,** *53*, 7549-7561.

[22] Kato, Y.; Inoue, K.; Kandori, H., Kinetic Analysis of H^+-Na^+ Selectivity in a Light-Driven Na^+-Pumping Rhodopsin. *J. Phys. Chem. Lett.* **2015,** *6* (24), 5111-5115.

[23] Kajimoto, K.; Kikukawa, T.; Nakashima, H.; Yamaryo, H.; Saito, Y.; Fujisawa, T.; Demura, M.; Unno, M., Transient Resonance Raman Spectroscopy of a Light-Driven Sodium-Ion-Pump Rhodopsin from *Indibacter alkaliphilus*. *J. Phys. Chem. B* **2017,** *121* (17), 4431-4437.

[24] Suomivuori, C. M.; Gamiz-Hernandez, A. P.; Sundholm, D.; Kaila, V. R. I.,

Energetics and dynamics of a light-driven sodium pumping rhodopsin. *Proc. Natl. Acad. Sci. U. S. A.* **2017,** *114* (27), 7043-7048.

[25] Kovalev, K.; Astashkin, R.; Gushchin, I.; Orekhov, P.; Volkov, D.; Zinovev, E.; Marin, E.; Rulev, M.; Alekseev, A.; Royant, A.; Carpentier, P.; Vaganova, S.; Zabelskii, D.; Baeken, C.; Sergeev, I.; Balandin, T.; Bourenkov, G.; Carpena, X.; Boer, R.; Maliar, N.; Borshchevskiy, V.; Büldt, G.; Bamberg, E.; Gordeliy, V., Molecular mechanism of light-driven sodium pumping. *Nat. Commun.* **2020,** *11* (1), 2137.

[26] Skopintsev, P.; Ehrenberg, D.; Weinert, T.; James, D.; Kar, R. K.; Johnson, P. J. M.; Ozerov, D.; Furrer, A.; Martiel, I.; Dworkowski, F.; Nass, K.; Knopp, G.; Cirelli, C.; Arrell, C.; Gashi, D.; Mous, S.; Wranik, M.; Gruhl, T.; Kekilli, D.; Brünle, S.; Deupi, X.; Schertler, G. F. X.; Benoit, R. M.; Panneels, V.; Nogly, P.; Schapiro, I.; Milne, C.; Heberle, J.; Standfuss, J., Femtosecond-to-millisecond structural changes in a light-driven sodium pump. *Nature* **2020,** *583* (7815), 314-318.

[27] Tamogami, J.; Kikukawa, T.; Miyauchi, S.; Muneyuki, E.; Kamo, N., A tin oxide transparent electrode provides the means for rapid time-resolved pH measurements: application to photoinduced proton transfer of bacteriorhodopsin and proteorhodopsin. *Photochem. Photobiol.* **2009,** *85* (2), 578-589.

[28] Hasemi, T.; Kikukawa, T.; Kamo, N.; Demura, M., Characterization of a Cyanobacterial Chloride-pumping Rhodopsin and Its Conversion into a Proton Pump. *J. Biol. Chem.* **2016,** *291* (1), 355-362.

[29] Nakamura, S.; Kikukawa, T.; Tamogami, J.; Kamiya, M.; Aizawa, T.; Hahn, M. W.; Ihara, K.; Kamo, N.; Demura, M., Photochemical characterization of actinorhodopsin and its functional existence in the natural host. *Biochim. Biophys. Acta Bioenerg.* **2016,** *1857* (12), 1900-1908.

[30] Hasemi, T.; Kikukawa, T.; Watanabe, Y.; Aizawa, T.; Miyauchi, S.; Kamo, N.; Demura, M., Photochemical study of a cyanobacterial chloride-ion pumping rhodopsin. *Biochim. Biophys. Acta Bioenerg.* **2019,** *1860* (2), 136-146.

[31] Kikukawa, T.; Kusakabe, C.; Kokubo, A.; Tsukamoto, T.; Kamiya, M.; Aizawa, T.; Ihara, K.; Kamo, N.; Demura, M., Probing the Cl--pumping photocycle of *pharaonis* halorhodopsin: Examinations with bacterioruberin, an intrinsic dye, and membrane potential-induced modulation of the photocycle. *Biochim. Biophys. Acta Bioenerg.* **2015,** *1847* (8), 748-758.

[32] Shibata, M.; Inoue, K.; Ikeda, K.; Konno, M.; Singh, M.; Kataoka, C.; Abe-Yoshizumi, R.; Kandori, H.; Uchihashi, T., Oligomeric states of microbial rhodopsins determined by high-speed atomic force microscopy and circular

dichroic spectroscopy. *Sci. Rep.* **2018,** *8* (1), 8262.

[33] Skulachev, V., A single turnover study of photoelectric current generating proteins. In *Method. Enzymol.*, Elsevier: 1982; Vol. 88, pp 35-45.

[34] Inoue, K.; Konno, M.; Abe-Yoshizumi, R.; Kandori, H., The Role of the NDQ Motif in Sodium-Pumping Rhodopsins. *Angew. Chem., Int. Ed.* **2015,** 54 (39), 11536-11539.

[35] Váró, G.; Lanyi, J. K., Effects of hydrostatic pressure on the kinetics reveal a volume increase during the bacteriorhodopsin photocycle. *Biochemistry* **1995,** *34* (38), 12161-12169.

[36] Kikukawa, T.; Saha, C. K.; Balashov, S. P.; Imasheva, E. S.; Zaslavsky, D.; Gennis, R. B.; Abe, T.; Kamo, N., The lifetimes of *pharaonis phoborhodopsin* signaling states depend on the rates of proton transfers - Effects of hydrostatic pressure and stopped flow experiments. *Photochem. Photobiol.* **2008,** *84* (4), 880-888.

[37] Shibasaki, K.; Shigemura, H.; Kikukawa, T.; Kamiya, M.; Aizawa, T.; Kawano, K.; Kamo, N.; Demura, M., Role of Thr218 in the light-driven anion pump halorhodopsin from *Natronomonas pharaonis*. *Biochemistry* **2013,** *52* (51), 9257-9268.

ACKNOWLEDGEMENTS

I gratefully acknowledge invaluable suggestion and support of Professor Makoto Demura, Lecture Takashi Kikukawa, and Assistant Professor Takashi Tsukamoto.

I would like to express my gratitude to Professor Tomoyasu Aizawa.

I deeply thank my colleagues for many advice, discussion, and kindness in my daily life. Finally, I would like to express grateful appreciation to my family for many support and encouragement during 9-years campus life in Hokkaido University.